Low-Pressure Plasma Polymer Modification from the FTIR Point of View

M. NITSCHKE, J. MEICHSNER

Technische Universität Chemnitz-Zwickau, Institut für Physik, D-09107 Chemnitz, Germany

Received 27 June 1996; accepted 30 December 1996

ABSTRACT: The main scope of this article was to demonstrate the potential of Fourier transform infrared (FTIR) spectroscopy as a diagnostic tool for low-pressure plasma polymer modification. Two model polymers, polyethylene and polystyrene, were treated in radio-frequency (rf) discharges in argon, hydrogen, oxygen, nitrogen, and tetrafluoromethane. *In situ* FTIR analysis was based on infrared reflection absorption spectroscopy (IRRAS) and attenuated total reflection (ATR). For both techniques, thin-film samples were prepared from polymer solution. The effects appearing in the infrared spectra are discussed. The results are compared with those from other diagnostic techniques. © 1997 John Wiley & Sons, Inc. J Appl Polym Sci **65:** 381–390, 1997

Key words: polymers; low-pressure plasma; infrared reflection absorption spectroscopy; attenuated total reflection

INTRODUCTION

Low-pressure plasma treatment of polymers is a widely used process to improve surface properties. Despite many applications, the complex phenomenon of plasma–wall interaction is not understood completely. A large number of elementary processes generates a wide variety of active particles (ions, electrons, radicals, metastable excited species) and vacuum ultraviolet radiation. The modification effects at the polymer surface observed as a result of low-pressure plasma treatment depend on the nature, flux, and energy distribution of the incident species. These values are governed by plasma bulk properties as well as by the transport mechanisms of charged particles in the plasma sheath.

Due to the small penetration depth of all involved processes, X-ray photoelectron spectroscopy (XPS) is the most frequently used tool for surface investigation. Beyond this, many other sophisticated methods like time of flight secondary ion mass spectroscopy, electron-induced vibrational spectroscopy, and photoacoustic spectroscopy were shown to be successful in polymer surface characterization.[1–3] Only few reports were given on the surface diagnostics of plasma-modified polymers by means of Fourier transform infrared (FTIR) spectroscopy, e.g., Refs. 4 and 5. Compared to photoelectron spectroscopy, this method provides additional information. But the potential of FTIR spectroscopy in this particular field cannot be exploited fully with standard sampling techniques. This is due to the need of *in situ* investigations and a lack of sensitivity and reproducibility of standard units. In this work, an effective approach to *in situ* diagnostics of low-pressure plasma polymer modification is introduced. The variety of observable effects is demonstrated for simple model substances.

The maximum penetration depth of the most significant primary processes in plasma–polymer interaction can be estimated from Monte Carlo calculations in the case of ions[6] and from polymer

Correspondence to: M. Nitschke at the Institut für Polymerforschung Dresden e. V., Hohe Str. 6, D-01069 Dresden, Germany. e-mail: nitschke@argos.ipfdd.de

Contract grant sponsor: BMBF.
Contract grant number: 13N6115.

Table I Experimental Parameters for the Preparation of 10–50 nm Polymer Films by Dip Coating

Polymer	Solvent	Concentration (%)	Temperature (°C)	Extraction Velocity (mm s^{-1})
Polyethylene	Toluene	0.1–1	72	1–15
Polystyrene	Trichoromethane	0.1–1	30	1–15

extinction coefficients in the case of vacuum ultraviolet (VUV) photons,[7,8] respectively. Assuming maximum ion energies in the range of some hundred electron volts and a considerable flux of VUV radiation ($\lambda < 160$ nm), the expected thickness of the modified surface layer is below 50 nm. Despite the fact that FTIR spectroscopy is not a surface-sensitive tool on this depth scale, thin-film ($d \approx 50$ nm) sampling techniques can lead to the required separation of bulk properties and surface effects.

EXPERIMENTAL

For the investigation of plasma-treated polymer surfaces, two *in situ* FTIR sampling techniques (infrared reflection absorption spectroscopy [IRRAS] and attenuated total reflection [ATR]) based on thin-film preparation were applied. For both techniques, special vacuum chambers were designed and placed in the sample compartment of a Bruker IFS66 FTIR spectrometer.

Polymer Film Preparation

Thin films of low-density polyethylene and polystyrene were prepared from solution by dip coating. Additive free polymers (Goodfellow, low-density polyethylene type ET31200, polystyrene type ST31080) were used as received. The principle of the dip coating technique is described in Ref. 9; the particular parameters for polyethylene and polystyrene are given in Table I.

The film thickness as a function of dip coating parameters (concentration and temperature of polymer solution, extraction velocity of the substrate) was measured by spectroscopic ellipsometry (ellipsometer S2000 by Rudolph Research) and correlated to IR band intensities. The homogeneity of the polymer films was checked by atomic force microscopy (Nanoscope 3 by Digital Instruments).

In this work, thin films were investigated instead of bulk samples due to restrictions of the analytical technique. For the generalization of results, it is necessary to prove the structural and chemical equivalence of bulk and film samples. This was done using FTIR spectroscopy, spectroscopic ellipsometry, and thermogravimetry.[10]

In Situ IRRAS Setup

In IRRAS, the IR beam of the spectrometer is reflected by a metal surface coated with a thin film of the sample material. Due to standing waves at the metal surface, an absorbing film of a thickness d ($d \ll \lambda$) is not detected in most cases. It was shown that a maximum absorption of a given film requires parallel polarization and a grazing incidence.[11,12] Under appropriate conditions, IRRAS spectra are very close to transmission spectra.[13] For the IRRAS experiments of this work, glass slides were metalized with gold by vacuum evaporation. On the gold surfaces, thin polymer films were prepared by dip coating.

The *in situ* IRRAS setup used for the experiments in this work is shown in Figure 1. A vacuum chamber contains two parallel electrodes (27 MHz radio frequency [rf], ground). Prismatic windows made of chalcogenide glass[14] deflect the IR beam by 15°. Depending on the orientation of the windows, the beam can be directed to the rf or to the grounded electrode. The resulting incident angle at the IRRAS sample placed at the electrode is 75°. This value is significantly below the optimum angle of 88°,[11] which cannot be realized with a typical beam divergence of $\approx 1°$ in the standard sample compartment of commercial FTIR spectrometers. For an incident angle of 75°, the sensitivity of the IRRAS technique drops to approximately 30% of the optimum case.[12]

The discharge was operated at an effective rf voltage $U_{\text{eff}} = 175$ V (level meter URV35 by Rohde & Schwarz). There was no gas flow during the short plasma treatment. The sample was

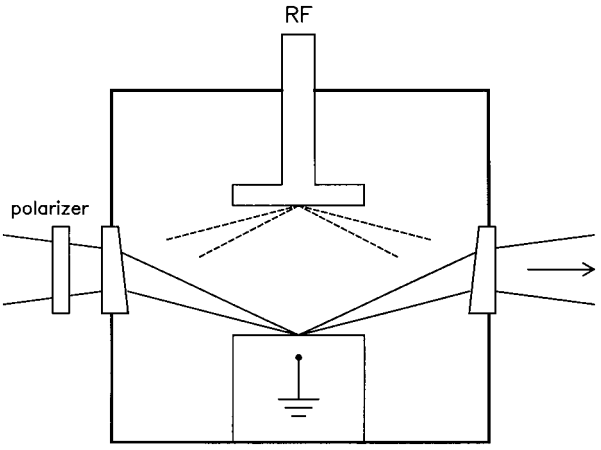

Figure 1 *In situ* IRRAS setup. By rotating the prismatic windows, the IR beam can be directed to a sample at the (· · · · · ·) rf or (——) grounded electrode, respectively.

placed at the grounded electrode for all examples of this work.

In Situ ATR Setup

The technique of ATR spectroscopy (internal reflection spectroscopy) is described in detail in Refs. 15 and 16. For ATR measurements, internal reflection elements (IRE) with a 45° incident angle and 34 reflections made of chalcogenide glass[14] were used.

A polymer film was prepared on one side of the IRE by dip coating. The coated IRE was integrated into the 27 MHz rf electrode of a plasma chamber as shown in Figure 2. The IRE is electrically insulated and the area directly faced to the plasma is mechanically limited. The effective number of reflections is restricted to 13. With a

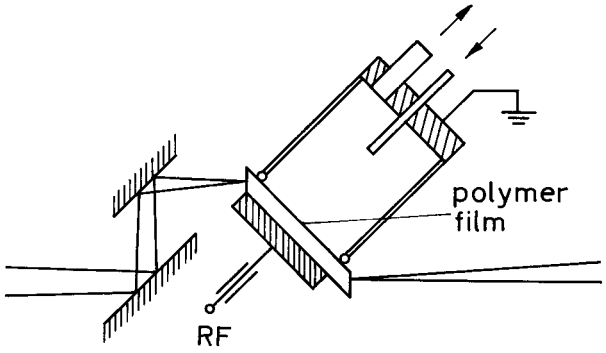

Figure 2 *In situ* ATR setup. The polymer film at the internal reflection element can be analyzed from one side while it is plasma treated from the other side.

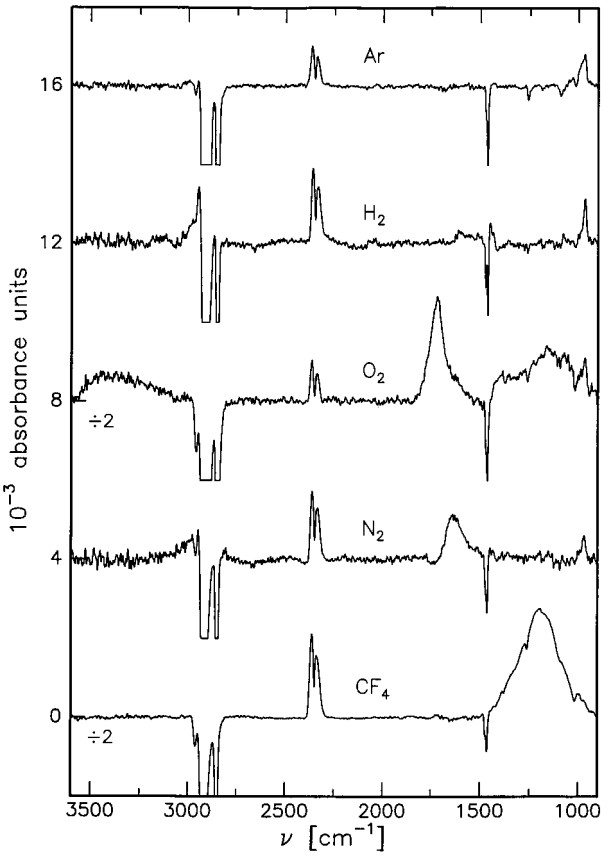

Figure 3 Plasma treatment of polyethylene (*in situ* ATR setup, $p = 5$ Pa, $t = 3$ s).

film thickness of 50 nm, the thin-film case of ATR spectroscopy ($d \ll \lambda$) applies.[15] The polymer film can be plasma-treated from one side and probed by FTIR from the other side. As in the case of the IRRAS setup, the discharge was operated at $U_{\text{eff}} = 175$ V (except the experiment of Fig. 3: $U_{\text{eff}} = 225$ V) without gas flow.

Chalcogenide glass, the material of the IRE, is nonhygroscopic and stable against attack by acids and organic solvents. Plasma etching of the IRE or plasma-surface reactions with the IRE material were beyond the detection limit under the experimental conditions of this work.

Ex Situ ATR Setup

In addition to the *in situ* ATR experiments, the same IRE were used for *ex situ* experiments (vertical ATR unit by Carl Zeiss Jena). In these experiments, the plasma treatment was performed in a reactor described in detail elsewhere.[17] In this setup, the energy distribution function of ions extracted directly from the plasma sheath at the

grounded electrode can be measured with a plasma monitor system (Hiden EQP300). An additional external DC bias voltage can be applied to shift the main peak of the ion-energy distribution within a wide range from some 10 to some 100 electron volts.

Postplasma Treatment

Additional information from the IR spectra can be obtained by chemical derivatization reactions, which are well known in photoelectron spectroscopy.[18–20] A gas-phase derivatization agent is applied to the plasma-exposed surface. In an *in situ* setup, the chemical labeling of a particular functional group can be monitored directly by FTIR. For the derivatization experiment described in this article, trifluoroacetic anhydride (TFAA, Aldrich, 99%) was used as received.

Measurement Procedure and Presentation of IR Spectra

All IR spectra in the following sections display exclusively *changes* at the polymer surface due to plasma treatment. The acquisition of these difference spectra is similar for all setups described above. First, a background spectrum I_0 is measured from the untreated polymer film (coated IRRAS substrate, coated IRE). In the next step, the polymer surface is exposed to the plasma and eventually posttreated by a derivatization agent. After this, the sample spectrum I is acquired. As a result, the absorbance spectrum $\log I_0/I$ displays the changes due to plasma exposure and chemical derivatization. While negative bands correspond to structures disappearing from the polymer sample, positive bands can be attributed to new surface species (for characteristic frequency tables, see Refs. 21 and 22).

Contrary to the *in situ* ATR setup, in the IRRAS setup, gas-phase species can contribute to the spectra. This is especially the case for fluorine-containing process gases like CF_4. For that reason, the IRRAS chamber is evacuated down to the base pressure of the vacuum system before measurements. For the *in situ* ATR setup, there is no need to evacuate the process gas. It is even possible to acquire spectra *during* the plasma treatment, but this was not done for the examples in this work.

All spectra were base line-corrected with the tools included in the spectrometer software. Bands originating from a variable concentration of water vapor in the IR ray path of the spectrometer outside the vacuum chamber were compensated. CO_2 bands from the same source at 2400–2280 cm^{-1} were not compensated. The intense bands of CH_2 stretching at 2950–2700 cm^{-1} were clipped in some cases for a better scaling of weak spectral features.

RESULTS AND DISCUSSION

Survey of IR Detectable Effects

To discuss the variety of IR detectable effects appearing as a result of plasma treatment, a set of overview spectra is displayed in Figure 3. In this experiment, polyethylene was treated in different plasmas. The modification effects were monitored with the ATR setup. Except for the process gas, all experimental parameters were kept constant.

Two general groups of modification effects can be distinguished: The effects of the first group are due to hydrogen abstraction, crosslinking, and ablation processes and show only slight variations for different plasmas. A second group of effects is characteristic for the particular plasma and involves the formation of structures containing foreign atoms.

Argon

As expected, the argon plasma treatment causes only effects of the first group. The negative bands at 2950–2700 and 1460 cm^{-1} (CH_2 stretching and bending) can be assigned to disappearing C—H structures, but the effects of the argon plasma treatment are not restricted to simple ablation processes. The positive band at 980–965 cm^{-1} (*trans*-vinylene CH wagging) indicates the formation of a surface layer with unsaturated structures. C≡C triple bonds (2270–2035) are not observed.

Hydrogen

In the case of hydrogen plasma, the spectrum shows the same features as described in the preceding paragraph. In addition, there are two positive bands at 3000–2950 and 1450–1410 cm^{-1}. The most probable interpretation are crosslinked hydrocarbon structures with an internal mechanical strain.[22]

Oxygen

A polymer treatment in an oxygen plasma results in a multitude of additional features from the sec-

ond group. These can be attributed to the formation of various oxygen-containing structures formed at the polymer surface. At 3600–3000 cm^{-1} appears the O—H stretching vibration of the hydroxyl group which is broadened due to hydrogen bonding. The carbonyl group is observed at 1800–1690 cm^{-1} (C=O stretching). The wide range covered by this vibration indicates a variety of C=O structures with slightly different characteristic frequencies. In the 1400–1000 cm^{-1} range, there are many overlapped bands associated with C—O stretching and O—H deformation in alcohols and C—O stretching in esters and ethers.

Nitrogen

In the case of nitrogen plasma treatment, the most prominent positive band is observed at 1725–1500 cm^{-1}. It can be assigned to the C=N stretching vibration. A possible contribution of C=C stretching cannot be disproved without additional information. A wide variety of structures as observed in the case of oxygen plasma is not evident after nitrogen plasma treatment. Even with the assumption that the weak vibration of hydrogen-bonded N—H at 3450–3250 cm^{-1} is not observable, the variety of nitrogen-containing species consistent with the observed spectral features is quite limited. Missing C—N stretching bands at 1190–1020 cm^{-1} disprove within the IR detection limit the presence of primary and secondary amines. These bands were also absent after treatment in stoichiometric N_2/H_2 plasmas, for which a formation of amine structures was reported by other authors.[23,24] The C≡N stretching vibration at 2260–2200 cm^{-1} is not observed.

Tetrafluoromethane

As seen in the bottom spectrum in Figure 3, the CF_4 plasma treatment of polyethylene results in a broad absorption band at 1400–1000 cm^{-1} associated with the C—F stretching vibration. The assignment of different fluorine-containing species is not possible under the experimental conditions of this work. The broad and overlapped spectral features of the CF_x species are caused by a strong coupling of the C—F vibration with vibrations of the polymer backbone.

Plasma Treatment of Polystyrene

The plasma-treatment experiments from Figure 3 were performed also for polystyrene. Under the same plasma conditions, the effects were very close to that of polyethylene. For all effects of the second group, similar band positions and band intensities were found. The positive bands in the CH stretching region attributed to a strained hydrocarbon network were more pronounced in the case of polystyrene. Possibly, this is due to plasma-induced ring opening as an additional source for such structures. The expected loss of aromaticity at the polystyrene surface was shown by other authors in similar plasma-treatment experiments by means of photoelectron spectroscopy.[25]

Experiments in Detail

Kinetics of Low-pressure Plasma Polymer Modification

After a time interval characteristic for the particular process, the concentration of structures formed at the polymer surface becomes stationary. An equilibrium of degradation and functionalization is established. Figure 4 shows this effect during oxygen and CF_4 plasma treatment of polyethylene. In both cases, the functional group concentration (i.e., the corresponding integrated band intensity) becomes stationary after a few seconds. For equal plasma parameters, the characteristic time constant of fluorination exceeds that of oxidation roughly by one order of magnitude. While the reaction velocity of carbonyl formation and the maximum concentration are increasing from 30 to 100 Pa, the corresponding values of CF_x are decreasing. The time-dependent loss of hydrocarbon structures is represented by the negative band intensity of the C—H stretching vibration. After a very short period, a linear behavior is observed.

Regarding these time dependencies, the maximum concentration of functional groups can be understood as the result of competing contributions from functionalization and degradation processes. This basic concept can be verified by other experimental techniques. Figure 5 shows the mass changes of a polyethylene sample measured *in situ* with an electronic microbalance during the fluorination in a CF_4 plasma.[26] In the first 20 s of the microgravimetric experiment, the mass of the polymer increases. This effect is due to the substitution of hydrogen and fluorine atoms during plasma treatment. The characteristic time constant is comparable to that from Figure 4. After reaching a particular level of fluorination, the

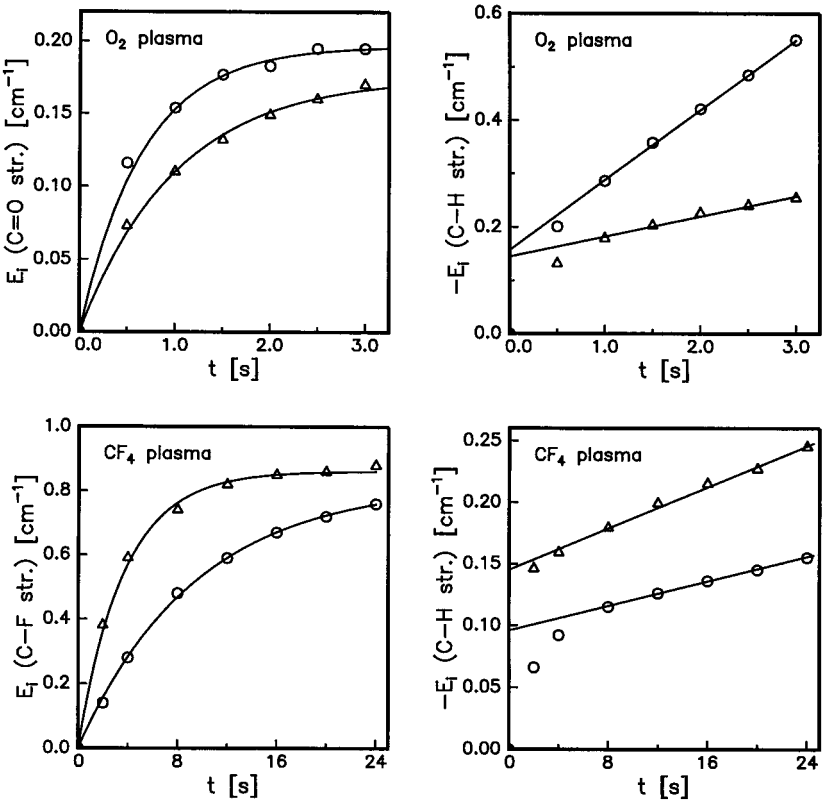

Figure 4 Time-dependent band intensities E_i during (top) oxygen plasma treatment and (bottom) CF_4 plasma treatment of polyethylene [*in situ* IRRAS setup, p = (△) 30 Pa and (○) 100 Pa]. Selected bands attributed to functionalization (C═O, C—F, left side) are compared with those attributed to degradation (C—H, right side).

overall degradation process becomes predominant and a linear mass decrease is observed. XPS investigations show a constant value of surface fluorine content during this phase.

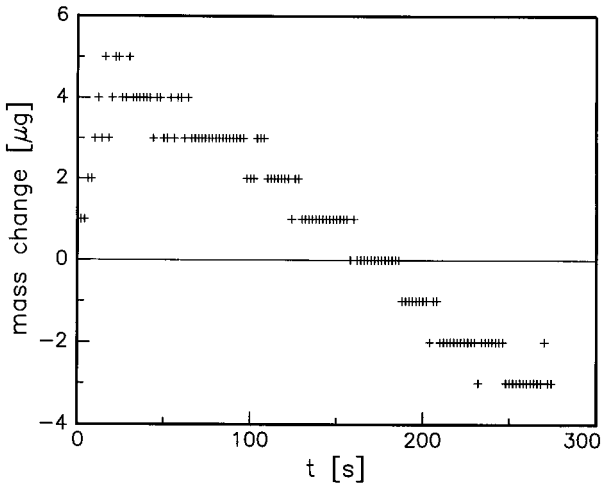

Figure 5 Mass change of a 900 mm^2 polyethylene foil during CF_4 plasma treatment (p = 20 Pa).

The process of polymer-surface functionalization is not limited to a simple increase of functional group concentration up to a certain level. It can be demonstrated that the composition of functional groups also changes during the subsaturation range of plasma treatment. As an example, Figure 6 shows the time-dependent behavior of the carbonyl peak during the oxygen plasma treatment of polyethylene. The peak appears at 1715 cm^{-1}. During the next few seconds, the total peak width increases while the maximum is shifted to higher wavenumbers.

Functional Group Formation Depending on Plasma Parameters

Concentration and composition of functional groups formed at the polymer surface during plasma treatment are expected to vary also with plasma conditions. The most dramatic changes in the plasma conditions should appear when the sample is moved from the plasma glow to a remote location downstream the gas flow.[27]

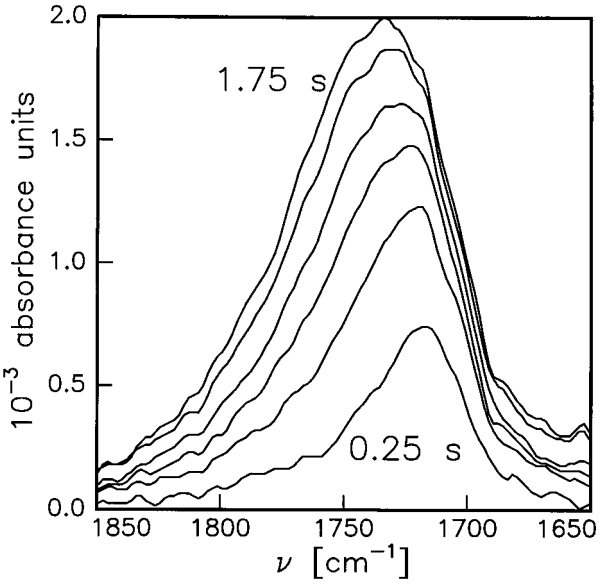

Figure 6 Time-dependent behavior of the C=O stretching vibration during oxygen plasma treatment of polyethylene (*in situ* IRRAS setup, p = 20 Pa, t = 0.25, 0.50–1.75 s).

The changes in the polymer surface layer are shown in Figure 7 for the case of oxygen plasma treatment of polyethylene. After 30 s of plasma treatment, the amount of oxygen-containing species reaches in both experiments a comparable level while the amount of disappeared hydrocarbon structures is lower by orders of magnitude in the case of the remote sample position. Beyond this, the most prominent difference is the band at 980–965 cm^{-1}, which was already attributed to C=C structures. This band is missing completely under remote plasma conditions, i.e., in the case of very low kinetic energy of impinging species. At least for this specific process, the formation of unsaturated structures seems to be correlated to high-energy particle bombardment.

Another difference between both experiments is the separation of particular bands in the 1400–1000 cm^{-1} range. These bands, related to a variety of oxygen-containing species, appear sharper and more separated in the remote plasma experiment. The most probable explanation for this effect is the following: A high-energy particle bombardment in the case of direct plasma treatment is accompanied by a high degree of disorder at the polymer surface. As a result, even in the case of a similar degree of oxydation, the chemical environment of a particular functional group is less uniform. In a less uniform environment, the IR bands of a given structure are broadened, which is observed in the experiment.

Preferential Degradation of Polymer Substructures

A polymer chain consists of several substructures. The reactivity of these substructures to the plasma species is expected to be different. So, the plasma attack to the polymer surface should be less or more efficient depending on the particular substructure.

The simplest example for a preferential polymer degradation is polyethylene with CH_2 units in the main chain and CH_3 units in end groups and side chains. To demonstrate the substructure-dependent efficiency of the plasma attack, three spectra from Figure 3 were normalized to equal intensities of the negative CH_2 stretching bands. The CH stretching region of the normalized spectra is redrawn in Figure 8. Contributions from CH_2 and CH_3 are indicated. The ratio of the integrated band intensities at 2920 and 2960 cm^{-1} is characteristic for the CH_3 content. In the absorption spectrum of polyethylene as used for this experiment, the ratio is equal to 12. A peak deconvolution in Figure 8 gives 70 for argon, 24 for oxygen, and 13 for CF_4. Obviously, the plasma attacks preferentially hydrogen attached to secondary carbon atoms while hydrogen attached to primary carbon atoms is more stable. With an increasing reactivity of the plasma species (Ar → F), the effect becomes less pronounced. Both tendencies are characteristic for a radical reaction in organic chemistry (e.g., halogenation of alkanes).

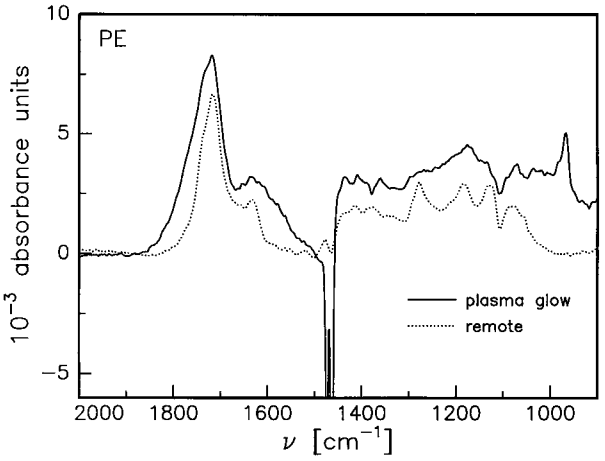

Figure 7 Oxygen plasma treatment of polyethylene. *Ex situ* ATR spectra for different sample positions: inside the plasma glow at the grounded electrode and 15 cm downstream (p = 3 Pa, t = 30 s).

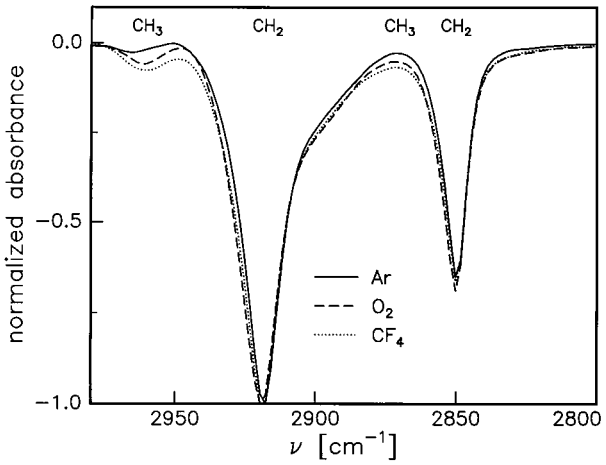

Figure 8 Degradation of CH_2 and CH_3 units in polyethylene in different plasmas (region redrawn from Fig. 3; spectra normalized to equal band intensity at 2920 cm^{-1}).

The example shows that these principles also apply to the plasma treatment of polymers.

Depth Profiles

The characteristic depth reached by different functionalization and degradation processes during low-pressure plasma polymer treatment is a controversely discussed subject. Analytical techniques like angle-resolved X-ray photoelectron spectroscopy (ARXPS),[1,28,29] Rutherford backscattering (RBS),[30] secondary ion mass spectroscopy (SIMS),[4] microgravimetry,[26] and gelation measurements[31] were used to determine depth profiles.

Most of these techniques give information on the depth profile of foreign atoms introduced during plasma treatment. Contrarily, from FTIR measurements, the depth profile of disappearing C—H structures can be derived. For this purpose, the following experiment was performed with the *in situ* IRRAS setup (Fig. 9): Polyethylene samples with different film thicknesses were plasma-treated for a constant time interval. The integrated band intensity E_i of the C—H stretching vibration was observed. When the penetration depth of the degradation process is less than the film thickness, the observed C—H loss does not vary with the film thickness. For film thicknesses less than the penetration depth, the observed C—H loss decreases. A penetration depth of about 10 nm is evident from Figure 9 for the case of hydrogen plasma (similar values for other plasmas). It should be mentioned here that due to the small reflection coefficients of metal surfaces in the VUV the plasma radiation does not cause standing waves at the sample position.

Chemical Derivatization

The information obtainable from IR spectra can be improved by chemical derivatization. For example, O—H stretching bands of hydroxyl groups formed during the oxygen plasma treatment of polymers are broadened due to hydrogen bonding. The corresponding C—O stretching and O—H deformation bands are overlapped by other spectral features. Even a semiquantitative interpretation is impossible under these circumstances. The labeling of hydroxyl groups with TFAA results in the formation of well-defined and separated bands.

Figure 10 shows the changes at a polyethylene surface during the oxygen plasma treatment and during a subsequent TFAA derivatization. In the upper part of Figure 10, the reaction scheme is given. The relations between the reactants and the corresponding spectral features are indicated. As expected, the broad O—H stretching band at 3600–3000 cm^{-1} is decreasing. New bands appear at 1250–1000 cm^{-1} (CF_3 stretching) and 1788 cm^{-1} (ester C=O stretching). Due to the vicinity of the CF_3 group, the ester carbonyl peak is well separated from the carbonyl peak of the plasma-treated polymer surface. As a side effect, the TFAA reaction causes a diminishing of the plasma-induced carbonyl band at 1726 cm^{-1}. The removal of low molecular weight products from

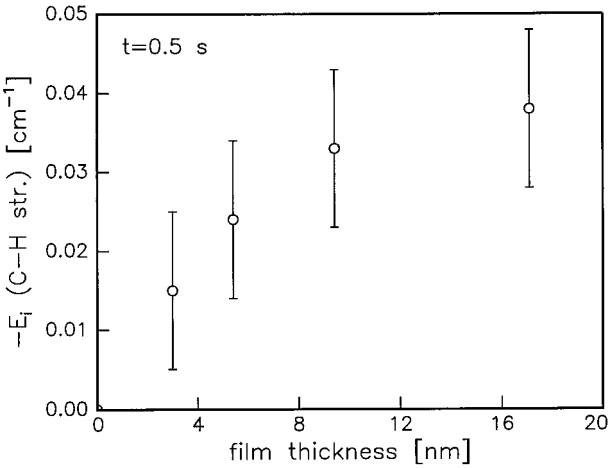

Figure 9 Loss of CH structures per time unit vs. film thickness during hydrogen plasma treatment of polyethylene (*in situ* IRRAS setup, p = 20 Pa, t = 0.5 s).

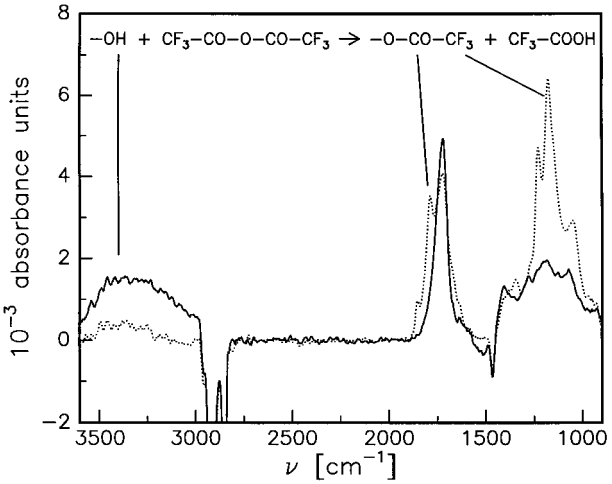

Figure 10 (——) Oxygen plasma treatment of polyethylene (*in situ* ATR setup, p = 50 Pa, t = 5 s) (· · ·) with subsequent TFAA derivatization (p = 50 Pa, t = 5 min).

the plasma treatment during the derivatization reaction is a possible explanation of this effect. For further details, especially the interpretation of derivatization reactions in terms of secondary structures, see Ref. 32.

CONCLUSIONS

With appropriate analytical techniques, it is possible to control concentration and composition of the species formed at the polymer surface during low-pressure plasma treatment. Infrared spectroscopy offers a number of advantages, but specific preparation and sampling techniques are necessary to separate surface properties from bulk properties. It was demonstrated that this can be done by reflection–absorption spectroscopy as well as by thin-film attenuated total reflection spectroscopy. Both sampling techniques can be performed *in situ*. Depending on the particular structure, sensitivities down to a submonolayer coverage are possible. For improved information about surface structures, the sample can be exposed with a gas-phase derivatization agent between plasma treatment and *in situ* FTIR investigation.

The variety of IR-detectable effects during low-pressure plasma polymer modification can be classified as follows: A first group of effects is attributed to hydrogen abstraction, crosslinking, and ablation and shows only slight variations for different plasmas. A second group includes all plasma-specific functionalization processes.

The potential of the introduced FTIR techniques is not limited to polymer modification. For example, structural gradients of plasma polymer films could be studied and controlled *in situ* during the deposition process.

REFERENCES

1. F. M. Petrat, D. Wolany, B. C. Schwede, L. Wiedmann, and A. Benninghoven, *Surf. Interf. Anal.,* **21,** 274 (1994).
2. L. Sabbatini and P. G. Zambonin, *Surface Characterization of Advanced Polymers,* VCH, Weinheim, 1993.
3. A. Garton, *Infrared Spectroscopy of Polymer Blends, Composits and Surfaces,* Hanser, Munich, 1992.
4. L. Leu and K. F. Jensen, *J. Vac. Sci. Technol.,* **A9,** 2948 (1991).
5. D. Dunn and D. J. McClure, *J. Vac. Sci. Technol.,* **A5,** 1327 (1987).
6. J. Ziegler, J. Biersack, and J. Littmark, *The Stopping and Range of Ions in Solids,* Pergamon Press, New York, 1985.
7. L. R. Painter, E. T. Arakawa, M. W. Williams, and J. C. Ashley, *Radiat. Res.,* **83,** 1 (1980).
8. J. G. Carter, T. N. Jelinek, R. N. Hamm, and R. D. Birkhoff, *J. Chem. Phys.,* **44,** 2266 (1966).
9. B. Cranfill, *Rev. Sci. Instrum.,* **49,** 264 (1978).
10. J. Meichsner, M. Arzt, J. Erben, M. Zeuner, M. Nitschke, R. Rochotzki, and A. Steinrücken, Report 13N6115, Federal Ministry of Research and Technology, Germany, 1993.
11. R. Greenler, *J. Chem. Phys.,* **44,** 310 (1966).
12. H. G. Tompkins, in *Methods of Surface Analysis,* A. W. Czanderna, Ed., Elsevier, Amsterdam, 1975.
13. D. L. Allara, A. Baca, and C. A. Pryde, *Macromolecules,* **11,** 1215 (1978).
14. P. Kloceck, *Handbook of Infrared Optical Materials,* Marcel Dekker, New York, 1991.
15. N. J. Harrick, *Internal Reflection Spectroscopy,* Interscience, New York, 1975.
16. Y. J. Chabal, *Internal Reflection Spectroscopy: Theory and Applications,* Marcel Dekker, New York, 1992.
17. M. Zeuner, J. Meichsner, and J. A. Rees, *J. Appl. Phys.,* **79,** 9379 (1996).
18. G. Allen and J. C. Bevington, Eds., *Comprehensive Polymer Science,* Pergamon Press, Oxford, 1989.
19. D. Briggs and M. P. Seah, *Practical Surface Analysis,* Wiley, New York, 1990, Vol. 1.
20. C. D. Batich, *Appl. Surf. Sci.,* **32,** 57 (1988).
21. G. Socrates, *Infrared Characteristic Group Frequencies: Tables and Charts,* Wiley, New York, 1994.

22. D. Lin-Vien, N. B. Colthup, W. G. Fately, and J. G. Grasseli, *The Handbook of Infrared and Raman Characteristic Frequencies of Organic Molecules,* Academic Press, New York, 1991.
23. R. Foerch, J. Izawa, and G. Separs, *J. Adhes. Sci. Technol.,* **5,** 549 (1991).
24. J. R. Hollahan and B. Stafford, *J. Appl. Polym. Sci.,* **13,** 807 (1969).
25. R. M. France and R. D. Short, *Polym. Degrad. Stab.,* **45,** 339 (1994).
26. J. Meichsner, M. Nitschke, R. Rochotzki, and M. Zeuner, *Surf. Coat. Technol.,* **74–75,** 227 (1995).
27. F. Normand, A. Granier, P. Leprince, J. Marec, M. K. Shi, and F. Clouet, *Plasma Chem. Plasma Process.,* **15,** 173 (1995).
28. R. Foerch, M. S. McIntyre, R. N. Sodhi, and D. H. Hunter, *J. Appl. Polym. Sci.,* **40,** 1903 (1990).
29. J. G. Terlingen, G. A. Takens, F. J. van der Gaag, A. S. Hoffman, and J. Feijen, *J. Appl. Polym. Sci.,* **52,** 39 (1994).
30. L. J. Matienzo, *J. Vac. Sci. Technol.,* **A6,** 950 (1988).
31. M. Hudis, *Polym. Lett.,* **10,** 179 (1972).
32. M. Nitschke, A. Holländer, F. Mehdorn, J. Behnisch, and J. Meichsner, *J. Appl. Polym. Sci.,* **59,** 119 (1996).